Materials Advances

ROYAL SOCIETY OF CHEMISTRY

PAPER

View Article Online
View Journal | View Issue

Cite this: *Mater. Adv.*, 2022, 3, 5941

A case of perfect convergence of light and heavy hole valence bands in SnTe: the role of Ge and Zn co-dopants

U. Sandhya Shenoy, *[a] Goutham K. D.[b] and D. Krishna Bhat *[c]

A dual step approach of decreasing the thermal conductivity and improving the power factor by using two different dopants has shown great promise in the development of high performance thermoelectrics. In this work, we dope Ge, which is well known to decrease the thermal conductivity of SnTe. Later, to this, we co-dope Zn to simultaneously improve the power factor. Zn, in the presence of Ge, introduces resonance levels, thus distorting the density of states near the Fermi level, improving the room temperature performance. In addition, it is also able to increase the band gap, thus preventing bipolar diffusion at high temperatures. The unique feature exhibited is the perfect convergence of light and heavy hole valence sub-bands achieved for the first time in SnTe promising a high performance throughout the temperature range. The transport property calculations reveal that in addition to p-type, it can also act as an outstanding n-type material by tuning its chemical potential, making it worth studying experimentally.

Received 19th March 2022,
Accepted 1st June 2022

DOI: 10.1039/d2ma00315e

rsc.li/materials-advances

1. Introduction

Thermoelectric materials and devices have become the heart of the energy conversion systems due to the rising demand for green energy technology. These materials provide solutions to the environmental crisis and energy needs by scavenging waste heat and converting it into electric current without release of harmful byproducts.[1–8] The extent to which a material can convert temperature difference into electric potential is decided by the figure of merit zT.[1,9] Research on SnTe- and GeTe-based materials has opened new avenues to develop a potential replacement for toxic PbTe-based thermoelectric materials.[4,10–15] SnTe, a rock salt analogue of PbTe, initially thought to be a poor thermoelectric material due to high carrier concentration and unfavorable electronic structure, is now at the forefront due to implementation of strategies like electronic structure and phonon band structure engineering to improve the power factor, while simultaneously decreasing the thermal conductivity.[16–42]

The Seebeck co-efficient of a material is directly proportional to the density of states (DOS) effective mass (m^*), which is a product of band effective mass (m_b) and number of degenerate valleys (N_v). Apart from high carrier concentration that increases the electrical and electronic thermal conductivity, a low Seebeck co-efficient resulting in poor thermoelectric performance arises due to the lower DOS effective mass due to non-participation of heavy hole valence bands in the transport due to higher energy offset between the light hole and heavy hole valence sub-bands. In order to decrease this energy-offset and increase the band degeneracy, several dopants such as Ag, Ca, Cd, Mg, Mo, V, and W have been used.[13,18–30] These dopants are also known to increase the band gap of SnTe leading to inhibition of the bipolar effect. The band effective mass (m_b) is also increased by distorting the DOS near the Fermi level by the addition of resonant dopants like In, Zn and Bi.[31–36] Among these, Zn is known to push the heavy hole valence band above the light hole valence band leading to its contribution for a broad temperature range.[15,18,35,36] On the other hand, dopants like Pb, Cu and Ge are used to decrease the thermal conductivity of SnTe.[37–42]

A dual step approach by decreasing the thermal conductivity by addition of Pb and improving the power factor by addition of a band convergent or a resonant dopant has been tried recently to improve the thermoelectric properties of SnTe leading to a record high room temperature zT of 0.35 at 300 K and a $ZT_{average}$ of 0.9 between 300 K and 840 K in Pb and Zn co-doped SnTe.[39,41] But due to the toxic nature of lead, finding an alternate set of co-dopants to induce the same beneficial features is of utmost importance. Herein, we use Ge alloying to reduce the thermal conductivity of SnTe and Zn to improve

[a] *Department of Chemistry, Institute of Engineering and Technology, Srinivas University, Mukka, Mangalore 574146, India. E-mail: sandhyashenoy347@gmail.com*
[b] *Indian Institute of Technology Guwahati, Guwahati 781039, Assam, India*
[c] *Department of Chemistry, National Institute of Technology Karnataka, Surathkal, Mangalore 575025, India. E-mail: denthajekb@gmail.com*

its power factor and study the electronic structure modifications. The simulated configuration of $Sn_9Ge_6ZnTe_{16}$ shows the introduction of resonance levels along with increased band gap and an interesting feature of a perfect convergence of light and heavy hole valence bands achieved for the first time in SnTe-based materials. The promising results obtained from transport property calculations make this material worth investigating experimentally.

2. Computational details

We simulated the electronic structures of SnTe, Ge-doped SnTe and Ge–Zn co-doped SnTe using the Quantum ESPRESSO package based on density functional theory (DFT).[43] A $(\sqrt{2} \times \sqrt{2} \times 2)a_o$ supercell was constructed with 32 atoms. DFT calculations were performed using relativistic pseudopotentials with the generalized gradient approximation to exchange the correlation energy with a functional type of Perdew–Burke–Erzenhoff (PBE).[44] As the atomic numbers of the elements involved were high, spin orbit coupling interactions were taken into consideration. The pseudopotentials considered ($4d^{10}5s^25p^2$), ($4d^{10}5s^25p^4$), ($3d^{10}4s^24p^2$) and ($3d^{10}4s^2$) as valence electrons in Sn, Te, Ge and Zn. Plane wave basis was used to represent the wavefunctions and the total energies were calculated for the fully relaxed supercells. 50 Ry and 400 Ry were used as cutoff values for the energy and charge density of the wavefunctions. A mesh of $14 \times 14 \times 10$ k points was used for the calculations. Electronic band structures were determined along the M–Γ–Z–R–A high symmetry path of the Brillouin zone.

3. Results and discussion

The band structure of a material plays a major role in its transport properties.[18,29] The electronic structure of $Sn_{16}Te_{16}$ displays a direct band gap of 0.08 eV at the Γ point; energy offsets of 0.30 eV and 0.24 eV were observed between the light hole and heavy hole valence bands and light electron and heavy electron conduction bands, respectively (Fig. 1(a)).[13,30] This explains the poor performance of the material due to non-participation of heavy carrier bands at $Z + \delta$ in the $Z \rightarrow R$ direction at lower temperatures and the onset of bipolar diffusion at higher temperatures due to the very small band gap. Due to the high carrier concentration as a result of Sn vacancies, SnTe is known to have high electronic thermal conductivity. This in addition to the high lattice thermal conductivity leads to high total thermal conductivity. In the quest for obtaining a lead-free high performance thermoelectric material, we alloy Ge in SnTe. We simulated a configuration of $Sn_{10}Ge_6Te_{16}$, which translates into ~37% alloying of Ge in SnTe experimentally, higher than the ~30% alloying of Pb used in the case of previous dual step approaches.[39,40] As the lattice mismatch is higher in the case of Pb doping to achieve similar defect scattering, a higher amount of Ge is essential. Although

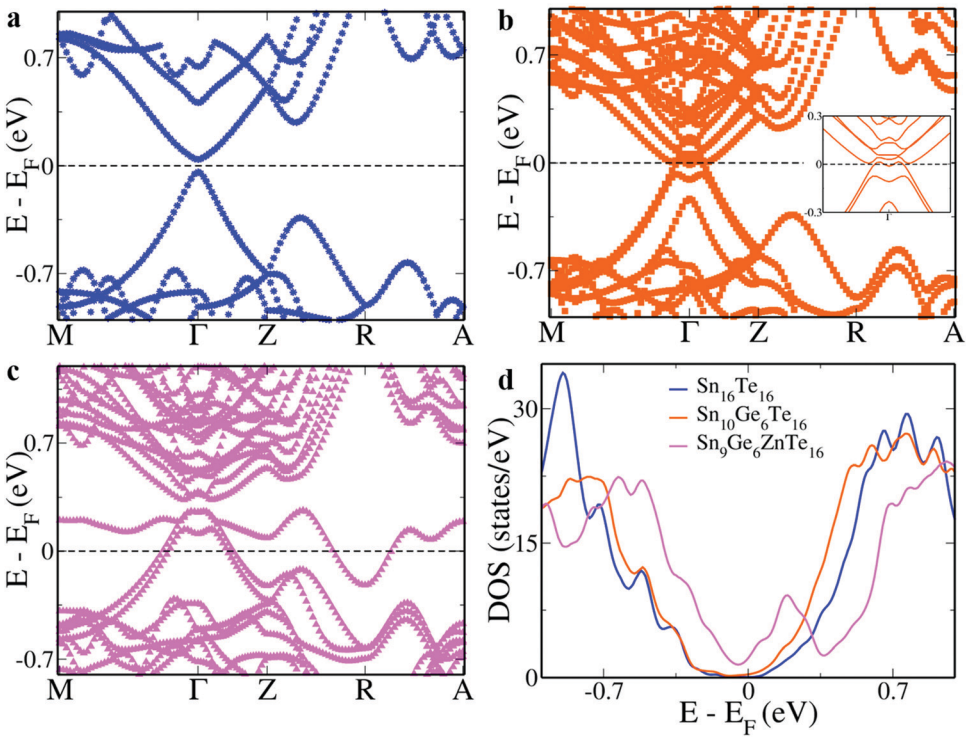

Fig. 1 Electronic structures of (a) $Sn_{16}Te_{16}$, (b) $Sn_{10}Ge_6Te_{16}$ and (c) $Sn_9Ge_6ZnTe_{16}$. (d) DOS plots of all three configurations. The appearance of a hump near the Fermi level in the DOS plot indicates the formation of a resonance level in $Sn_9Ge_6ZnTe_{16}$. The energy levels are shifted with respect to the Fermi level, which is set to zero. The L point of the primitive cell folds onto the Γ point and the Σ point folds onto the $Z + \delta$ in the $Z \rightarrow R$ direction in the current supercell.

alloying of Ge decreases the thermal conductivity as reported previously, it deteriorates the power factor at higher temperatures due to the bipolar effect.[45] The electronic structure reveals a negligible band gap, which results in the diffusion of minority carriers across the band gap decreasing the Seebeck values at higher temperatures (Fig. 1(b)). In addition, these carriers also transport heat leading to an increase in the bipolar thermal conductivity as in the case of TCI material $Pb_{10}Sn_6Te_{16}$.[46,47] The p-type transport is further affected as the energy gap between the valence sub-bands at the Γ and $Z+\delta$ point further increases to 0.35 eV. The increase in the separation of the valence sub-bands in the case of Ge alloying is seen to be higher than that in the case of Pb alloying reported previously.[41]

Hence, in order to improve the power factor, we introduced Zn into the above system. The electronic structure of $Sn_9Ge_6ZnTe_{16}$ reveals a band gap of 0.12 eV at the Γ point (Fig. 1(c)). The interesting feature here is the perfect convergence of light and heavy hole valence bands never achieved before *via* any other dopant combination leading to the participation of 16 degenerate valleys (4 from Γ point and 12 from $Z+\delta$ point) in the transport at room temperature. This increase in the number of degenerate valleys (N_v) increases the effective mass of the carrier without effecting the carrier mobility.[1] It is also observed that the energy-offset between the conduction sub-bands decreases from 0.20 eV in $Sn_{10}Ge_6Te_{16}$ to 0.13 eV in $Sn_9Ge_6ZnTe_{16}$ enabling a better performance in a Fermi level tuned n-type scenario.[29,47] The comparison of the total DOS reveals a peak closer to the Fermi level indicating the formation of a resonance level in Ge–Zn co-doped SnTe (Fig. 1(d)).[35,36] This resonance level appears to cap the valence band edge at the Γ point, primarily formed from the uppermost doubly degenerate valence band. Doping of Ge results in the breaking of eight-fold degenerate bands into a four-fold band and two sets of doubly degenerate bands all lying within $\sim$0.3 eV of each other. Co-doping of Zn leads to further splitting of the topmost 4-fold degenerate band into two sets of doubly degenerate bands with the uppermost one forming the resonance level. The difference in the electronic structure of the previously reported Pb–Zn co-doped system and Ag/Ca/Mg–Zn co-doped system with the present Ge–Zn co-doped system is that although Zn introduces p-type resonance levels leading to distortion in the DOS in all the cases mentioned, in the previously reported cases it led to hyperconvergence of the heavy hole valence bands, while in the present case it leads to perfect convergence.[18,39] This indicates that the effect of a dopant in engineering the electronic structure depends predominantly on the presence of other co-dopants in the system. Hence, the present work not only reports a lead-free combination of dopants to improve the thermoelectric properties of SnTe, but also reports a new approach to achieve perfect convergence, highlighting the significance of the co-dopant in electronic structure engineering.

When we projected the atomic orbitals onto the DOS, we observed that in the case of both $Sn_{10}Ge_6Te_{16}$ and $Sn_9Ge_6ZnTe_{16}$ the valence band is primarily formed by the Te 'p' orbitals, while the conduction bands by Sn 'p' orbitals similar to SnTe (Fig. 2).[33] Furthermore, Ge alloying leads to the conduction band edges formed typically out of 'p' states of Ge. Substitutional doping of Zn in the Sn site leads to an increase in DOS near the Fermi level resulting in the formation of deep defect levels around $\sim$0 eV and hyper-deep defect levels ~ -4.5 eV.[35] The formation of resonance levels is known to improve the room temperature Seebeck values resulting in improved average *ZT* throughout the temperature range.[36,39]

We studied the transport properties, namely the electrical conductivity 'σ', Seebeck co-efficient 'S', power factor 'σS^2' and thermal conductivity 'κ' as a function of chemical potential 'μ' using the Boltztrap code.[48] A rigid band and a constant scattering time approximation were considered during the study in the temperature range of 300 to 800 K as reported previously.[29,30,41] Using eqn (1) and (2), we determined the electrical conductivity and the Seebeck coefficient.[30,49]

$$\sigma_{\alpha\beta}(T, E_F) = \frac{1}{\Omega}\int \Sigma_{\alpha\beta}(\varepsilon)\left[-\frac{\delta f_0(T, \varepsilon, E_F)}{\delta\varepsilon}\right]d\varepsilon \quad (1)$$

$$S_{\alpha\beta}(T, E_F) = \frac{1}{eT\sigma_{\alpha\beta}(T, E_F)}\int (\varepsilon - E_F)\Sigma_{\alpha\beta}(\varepsilon)\left[-\frac{\delta f_0(T, \varepsilon, E_F)}{\delta\varepsilon}\right]d\varepsilon \quad (2)$$

where α and β are the Cartesian indices, Ω is the unit cell volume, f_0 is the Fermi–Dirac distribution function of the carriers and $\Sigma_{\alpha\beta}$ is the transport distribution function.[30,49]

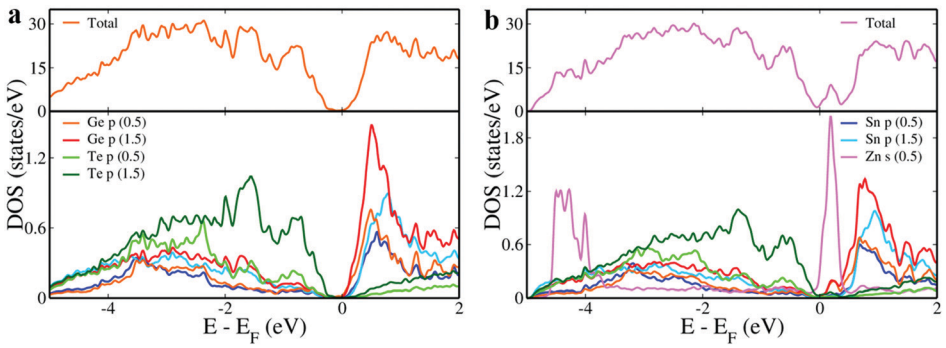

Fig. 2 pDOS of (a) $Sn_{10}Ge_6Te_{16}$ and (b) $Sn_9Ge_6ZnTe_{16}$. The energy levels are shifted with respect to the Fermi level of the configurations, which is set to zero.

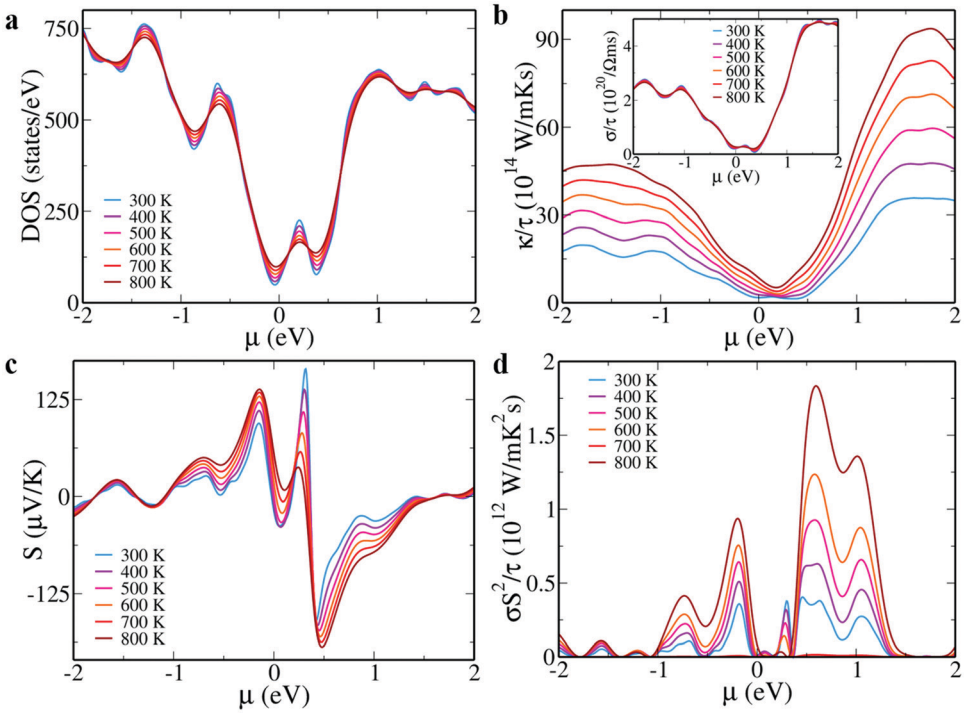

Fig. 3 (a) DOS, (b) thermal conductivity (inset: electrical conductivity), (c) Seebeck co-efficient and (d) power factor of $Sn_9Ge_6ZnTe_{16}$ as a function of chemical potential (μ) at various temperatures. The conductivity and power factor values are reported by scaling them with τ.

We observe the decrease in the intensity of the resonance peak with increase in the temperature, which is a classic sign of the diminishing resonance effect due to the increase in the relaxation time of the resonant impurity scattering in comparison to the acoustic phonon scattering (Fig. 3(a)).[1] While 'σ' does not seem to vary much with the temperature change, 'κ' is seen to increase with increase in temperature with higher values for positive potentials (Fig. 3(b)). As we move from negative potential representing p-type doping to positive potential representing n-type doping, the sign of the 'S' value changes from positive to negative (Fig. 3(c)).[29,30] Fig. 3(d) shows four prominent peaks in 'σS^2' values with two each on either side of the Fermi level indicating that the material could be tuned to act as either p-type or n-type depending on where the Fermi level resides.[41]

While the perfect convergence of valence sub-bands and distortion in DOS leads to an improved p-type material, the convergence of conduction sub-bands leads to a potential n-type material in SnTe by tuning the Fermi level.[50] These features in addition to the increased band gap showcase the perfect tuning of the electronic structure due to co-doping of Ge and Zn in SnTe. Zn, which is well known to cause hyperconvergence, deviates from its regular behavior in the presence of Ge. This feature points towards the fact that the right combination of dopants is highly essential to achieve the desired properties.[33,36,41] In addition, the co-doping strategy is also known to decrease the thermal conductivity due to the increased scattering of phonons.[18,36,39] Since both SnTe and GeTe have inherent cation vacancies, self-compensation in the form of addition of excess Sn/Ge is well known to tune the carrier concentration.[21,24,51] Hence, this work promotes an experimental study on SnTe by alloying 40 mol% Ge (3 mol% to reduce the vacancies and 37% for achieving the desired configuration mentioned in the theoretical study) with up to 6 mol% Zn doping to realize a high performing thermoelectric material free from toxic lead.

4. Conclusions

Herein, we use a dual step approach of Ge doping to reduce the thermal conductivity of SnTe and Zn doping to improve its power factor. We see that apart from increasing the band gap and the introduction of resonance levels, Zn in the presence of Ge as a co-dopant enables a perfect convergence of light and heavy hole valence sub-bands. While distortion of the density of states near the Fermi level by Zn increases the room temperature Seebeck values, increase in the band gap prevents the early onset of the bipolar effect, thus increasing the Seebeck values at high temperatures also. The perfect convergence of the valence bands leads to an increase in the number of valleys contributing to the transport throughout the temperature range. The electronic structure reveals the potential of the unique combination of Ge and Zn dopants in SnTe in thermoelectric applications, which is further supported by the Boltzmann transport calculations. Thus, this work acts as a new approach for producing lead-free thermoelectric materials with promising thermoelectric properties, which is worth exploring further experimentally.

Conflicts of interest

The authors declare no competing financial interest.

Acknowledgements

The authors gratefully acknowledge financial support received from CSIR, Govt. of India in the form of an R&D project grant and DST, Govt. of India for an INSPIRE Faculty award.

References

1 G. Tan, L. D. Zhao and M. G. Kanatzidis, Rationally designing high-performance bulk thermoelectric materials, *Chem. Rev.*, 2016, **116**, 12123–12149.
2 X. L. Shi, J. Zou and Z. G. Chen, Advanced thermoelectric design: From materials and structures to devices, *Chem. Rev.*, 2020, **120**, 7399–7515.
3 U. S. Shenoy and D. K. Bhat, Vanadium doped $BaTiO_3$ as high performance thermoelectric material: Role of electronic structure engineering, *Mater. Today Chem.*, 2020, **18**, 100384.
4 Y. Zhang, J. Sun, J. Shuai, X. Tang and G. Tan, Lead-free SnTe-based compounds as advanced thermoelectrics, *Mater. Today Phys.*, 2021, **19**, 100405.
5 T. Zilber, S. Cohen, D. Fuks and Y. Gelbstein, TiNiSn Half-Heusler crystals grown from metallic flux for thermoelectric applications, *J. Alloys Compd.*, 2019, **781**, 1132–1138.
6 O. Meroz and Y. Gelbstein, Thermoelectric $Bi_2Te_{3-x}Se_x$ alloys for efficient thermal to electrical energy conversion, *Phys. Chem. Chem. Phys.*, 2018, **20**, 4092–4099.
7 Y. Sadia, M. Elegrably, O. Ben-Nun, Y. Marciano and Y. Gelbstein, Sub-micron features in higher manganese silicide, *J. Nanomater.*, 2013, 701268.
8 U. S. Shenoy and D. K. Bhat, Electronic structure engineering of $SrTiO_3$ *via* rhodium doping: A DFT study, *J. Phys. Chem. Solids*, 2021, **148**, 109708.
9 Y. Sadia, T. Ohaion-Raz, O. Ben-Yehuda, M. Korngold and Y. Gelbstein, Criteria for extending the operation periods of thermoelectric converters based on IV–VI cOmpounds, *J. Solid State Chem.*, 2016, **241**, 79–85.
10 B. Dado, Y. Gelbstein and M. P. Dariel, Nucleation of nano-size particles following the spinodal decomposition in The Pseudo-Ternary $Ge_{0.6}Sn_{0.1}Pb_{0.3}Te$ compound, *Scr. Mater.*, 2010, **62**, 89–92.
11 D. K. Bhat and U. S. Shenoy, Mg/Ca doping ameliorates the thermoelectrics properties of GeTe: Influence of electronic structure engineering, *J. Alloys Compd.*, 2020, **834**, 155989.
12 T. Wang, C. Zhang, J. Y. Yang and L. Liu, Engineering the electronic band structure and thermoelectric performance of GeTe *via* lattice structure manipulation from first-principles, *Phys. Chem. Chem. Phys.*, 2021, **23**, 23576–23585.
13 U. S. Shenoy, D. K. Goutham and D. K. Bhat, Resonance states and hyperconvergence induced by tungsten doping in SnTe: Multiband transport leading to a propitious thermoelectric material, *J. Alloys Compd.*, 2022, **905**, 164146.
14 H. T. Liu, Q. Sun, Y. Zhong, C. L. Xia, Y. Chen, Z. G. Chen and R. Ang, Achieving high performance n-type PbTe *via* synergistically optimizing effective mass and carrier concentration and suppressing lattice thermal conductivity, *Chem. Eng. J.*, 2022, **428**, 132601.
15 U. S. Shenoy and D. K. Bhat, Electronic structure modulation of $Pb_{0.6}Sn_{0.4}Te$ *via* zinc doping and its effect on the thermoelectric properties, *J. Alloys Compd.*, 2021, **872**, 159681.
16 N. Jia, J. Cao, X. Y. Tan, J. Dong, H. Liu, C. K. I. Tan, J. Xu, Q. Yu, X. J. Loh and A. Suwardi, Thermoelectric materials and transport physics, *Mater. Today Phys.*, 2021, **21**, 100519.
17 Q. Yang, T. Lyu, Y. Dong, B. Nan, J. Tie, X. Zhou, B. Zhang and G. Xu, Anion exchanged Cl doping achieving band sharpening and low lattice thermal conductivity for improving thermoelectric performance in SnTe, *Inorg. Chem. Front.*, 2021, **8**, 4666–4675.
18 U. S. Shenoy and D. K. Bhat, Selective Co-doping improves the thermoelectric performance of SnTe: An outcome of electronic structure engineering, *J. Alloys Compd.*, 2021, **892**, 162221.
19 R. Moshwan, W. D. Liu, X. L. Shi, Q. Sun, H. Gao, Y. P. Wang, J. Zou and Z. G. Chen, Outstanding thermoelectric properties of solvothermal-synthesized $Sn_{1-3x}In_xAg_{2x}Te$ micro-crystals through defect engineering and band tuning, *J. Mater. Chem. A*, 2020, **8**, 3978–3987.
20 A. Banik, U. S. Shenoy, S. Saha, U. V. Waghmare and K. Biswas, High power factor and enhanced thermoelectric performance of $SnTe$-$AgInTe_2$: Synergistic effect of resonance level and valence band convergence, *J. Am. Chem. Soc.*, 2016, **138**, 13068–13075.
21 D. K. Bhat and U. S. Shenoy, Enhanced thermoelectric performance of bulk tin telluride: Synergistic effect of calcium and indium Co-doping, *Mater. Today Phys.*, 2018, **4**, 12–18.
22 G. Tan, L. D. Zhao, F. Shi, J. W. Doak, S. H. Lo, H. Sun, C. Wolverton, V. P. Dravid, C. Uher and M. G. Kanatzidis, High thermoelectric performance of p-type SnTe *via* a synergistic band engineering and nanostructuring approach, *J. Am. Chem. Soc.*, 2014, **136**, 7006–7017.
23 M. Ibanez, R. Hasler, A. Genc, Y. Liu, B. Kuster, M. Schuster, O. Dobrozhan, D. Cadavid, J. Arbiol, A. Cabot and M. V. Kovalenko, Ligand mediated band engineering in bottom-up assembled SnTe Nanocomposites for thermoelectric energy conversion, *J. Am. Chem. Soc.*, 2019, **141**, 8025–8029.
24 D. K. Bhat and U. S. Shenoy, High thermoelectric performance of Co-doped tin telluride due to synergistic effect of magnesium and indium, *J. Phys. Chem. C*, 2017, **121**, 7123–7130.
25 J. Wang, Y. Yu, J. He, J. Wang, B. Ma, X. Chao, Z. Yang and D. Wu, Synergy of valence band modulation and grain boundary engineering leading to improved thermoelectric performance in SnTe, *ACS Appl. Energy Mater.*, 2021, **4**, 14608–14617.
26 A. Banik, U. S. Shenoy, S. Anand, U. V. Waghmare and K. Biswas, Mg alloying in SnTe facilitates valence band convergence and optimizes thermoelectric properties, *Chem. Mater.*, 2015, **27**, 581–587.

27 S. K. Kihoi, J. N. Kahiu, H. Kim, U. S. Shenoy, D. K. Bhat, S. Yi and H. S. Lee, Optimized Mn and Bi Co-doping in SnTe based thermoelectric material: A case of band engineering and density of states tuning, *J. Mater. Sci. Technol.*, 2021, **85**, 76–86.

28 X. Xu, J. Cui, L. Fu, Y. Huang, Y. Yu, Y. Zhou, D. Wu and J. He, Enhanced thermoelectric performance achieved in SnTe *via* the synergy of valence band regulation and Fermi level modulation, *ACS Appl. Mater. Interfaces*, 2021, **13**, 50037–50045.

29 U. S. Shenoy and D. K. Bhat, Molybdenum as a versatile dopant in SnTe: A promising material for thermoelectric application, *Energy Adv.*, 2022, **1**, 9–14.

30 U. S. Shenoy and D. K. Bhat, Vanadium: A protean dopant in snte for augmenting its thermoelectric performance, *ACS Sustainable Chem. Eng.*, 2021, **9**, 13033–13038.

31 Q. Yang, T. Lyu, Z. Li, H. Mi, Y. Dong, H. Zheng, Z. Sun, W. Feng and G. Xu, Realizing widespread resonance effects to enhance thermoelectric performance of SnTe, *J. Alloys Compd.*, 2021, **852**, 156989.

32 S. K. Kihoi, U. S. Shenoy, D. K. Bhat and H. S. Lee, Complimentary effect of Co-doping aliovalent elements Bi and Sb in self-compensated SnTe-based thermoelectric materials, *J. Mater. Chem. C*, 2021, **9**, 9922–9931.

33 U. S. Shenoy and D. K. Bhat, Electronic structure engineering of tin telluride through Co-doping of bismuth and indium for high performance thermoelectrics: A synergistic effect leading to record high room temperature *ZT* in tin telluride, *J. Mater. Chem. C*, 2019, **7**, 4817–4821.

34 S. Song, Z. Yang, Y. Huang, Y. C. Tseng, S. M. Valiyaveettil, K. H. Chen and Y. Mozharivskyj, Enhancing thermoelectric performance of $Sn_{0.5}Ge_{0.5}Te$ *via* doping with In/Zn, In/Sb and In/Bi, *J. Solid State Chem.*, 2021, **302**, 122444.

35 D. K. Bhat and U. S. Shenoy, Zn: A versatile resonant dopant for SnTe THermoelectrics, *Mater. Today Phys.*, 2019, **11**, 100158.

36 U. S. Shenoy and D. K. Bhat, Bi and Zn Co-doped SnTe thermoelectrics: Interplay of resonance levels and heavy hole band dominance leading to enhanced performance and a record high room temperature *ZT*, *J. Mater. Chem. C*, 2020, **8**, 2036–2042.

37 X. Wang, H. Yao, Z. Zhang, X. Li, C. Chen, L. Yin, K. Hu, Y. Yan, Z. Li, B. Yu, F. Cao, X. Liu, X. Lin and Q. Zhang, Enhanced thermoelectric performance in high entropy alloys $Sn_{0.25}Pb_{0.25}Mn_{0.25}Ge_{0.25}Te$, *ACS Appl. Mater. Interfaces*, 2021, **13**, 18638–18647.

38 J. Tang, Z. Yao, Y. Wu, S. Lin, F. Xiong, W. Li, Y. Chen, T. Zhu and Y. Pei, Atomic disordering advances thermoelectric group IV telluride alloys with a multi-band transport, *Mater. Today Phys.*, 2020, **15**, 100247.

39 D. K. Bhat and U. S. Shenoy, SnTe Thermoelectrics: Dual step approach for enhanced performance, *J. Alloys Compd.*, 2020, **834**, 155181.

40 S. Roychowdhury, S. U. Shenoy, U. V. Waghmare and K. Biswas, An enhanced seebeck coefficient and high thermoelectric performance in p-type In and Mg co-doped $Sn_{1-x}Pb_xTe$ via the co-adjuvant effect of the resonance level and heavy hole valence band, *J. Mater. Chem. C*, 2017, **5**, 5737–5748.

41 U. S. Shenoy and D. K. Bhat, Improving *ZT* of SnTe by electronic structure engineering: Unusual behavior of Bi dopant in the presence of Pb as a Co-dopant, *Mater. Adv.*, 2021, **2**, 6267–6271.

42 G. Wu, Z. Guo, Q. Zhang, X. Wang, L. Chen, X. Tan, P. Sun, G. Q. Liu, B. Yu and J. Jiang, Refined band structure plus enhanced phonon scattering realizes thermoelectric performance optimization in Cu–Mn Co-doped SnTe, *J. Mater. Chem. A*, 2021, **9**, 13065–13070.

43 P. Giannozzi, S. Baroni, N. Bonini, M. Calandra, R. Car, C. Cavazzoni, D. Ceresoli, G. L. Chiarotti, M. Cococcioni and I. Dabo, *et al.*, Quantum ESPRESSO: A modular and open-source software project for quantum simulations of materials, *J. Phys.: Condens. Matter*, 2009, **21**, 395502.

44 J. P. Perdew, K. Burke and M. Ernzerhof, Generalized gradient approximation made simple, *Phys. Rev. Lett.*, 1996, **77**, 3865.

45 T. J. Slade, K. Pal, J. A. Grovogui, T. P. Bailey, J. Male, J. F. Khoury, X. Zhou, D. Y. Chung, G. J. Snyder, C. Uher, V. P. Dravid, C. Wolverton and M. G. Kanatzidis, Contrasting SnTe–$NaSbTe_2$ and SnTe–$NaBiTe_2$ Thermoelectric alloys: High performance facilitated by increased cation vacancies and lattice softening, *J. Am. Chem. Soc.*, 2020, **142**, 12524–12535.

46 S. Shenoy and D. K. Bhat, Enhanced bulk thermoelectric performance of $Pb_{0.6}Sn_{0.4}Te$: Effect of magnesium doping, *J. Phys. Chem. C*, 2017, **121**, 20696–20703.

47 U. S. Shenoy and D. K. Bhat, Halide (X = I, Br, Cl) doping to tune the electronic structure for conversion of Pb0.6Sn0.4Te into a high performing thermoelectric material, *Energy Adv.*, 2022, **1**, 15–20.

48 G. K. H. Madsen and D. J. Singh, BoltzTrap. A code for calculating band structure dependent quantities, *Comput. Phys. Commun.*, 2006, **175**, 67–71.

49 U. S. Shenoy and D. K. Bhat, Enhanced thermoelectric properties of vanadium doped $SrTiO_3$: A resonant dopant approach, *J. Alloys Compd.*, 2020, **832**, 154958.

50 H. Pang, Y. Qiu, D. Wang, Y. Qin, R. Huang, Z. Yang, X. Zhang and L. D. Zhao, Realizing n-type SnTe thermoelectrics with competitive performance through suppressing Sn VACancies, *J. Am. Chem. Soc.*, 2021, **143**, 8538–8542.

51 D. K. Bhat and U. S. Shenoy, Resonance levels in GeTe thermoelectrics: Zinc as a new multifaceted dopant, *New J. Chem.*, 2020, **44**, 17664–17670.